



UNIVERSITÀ DI PARMA

ARCHIVIO DELLA RICERCA

This is the peer reviewed version of the following article:

Original

Cucurbit[7]uril-Dimethyllysine Recognition in a Model Protein / Guagnini, Francesca; Antonik, Pawe M.; Rennie, Martin L.; O'Byrne, Peter; Khan, Amir R.; Pinalli, Roberta; Dalcanale, Enrico; Crowley, Peter B.. - In: ANGEWANDTE CHEMIE. INTERNATIONAL EDITION. - ISSN 1433-7851. - 57:24(2018), pp. 7126-7130. [10.1002/anie.201803232]

Availability:

This version is available at: 11381/2847713 since: 2021-10-02T18:14:17Z

Publisher:

Wiley-VCH Verlag

Published

DOI:10.1002/anie.201803232

Terms of use:

Open Access

Anyone can freely access the full text of works made available as "Open Access". Works made available under a Creative Commons license can be used according to the terms and conditions of said license. Use of all other works requires consent of the right holder (author or publisher) if not exempted from copyright protection by the applicable law.

When citing, please refer to the published version.

(Article begins on next page)

Cucurbit[7]uril–Dimethyllysine Recognition in a Model Protein

Francesca Guagnini,^{[a][b]} Paweł M. Antonik,^[a] Martin L. Rennie,^[a] Peter O'Byrne,^[c] Amir R. Khan,^[c] Roberta Pinalli,^[b] Enrico Dalcanale,^[b] and Peter B. Crowley^{*[a]}

Abstract: Here, we provide the first structural characterization of host-guest complexation between cucurbit[7]uril (**Q7**) and dimethyllysine (KMe₂) in a model protein. Binding was dominated by complete encapsulation of the dimethylammonium functional group. While selectivity for the most sterically accessible dimethyllysine was observed both in solution and in the solid state, three different modes of **Q7**–KMe₂ complexation were revealed by X-ray crystallography. The crystal structures revealed also entrapped water molecules that persisted in solvating the ammonium group within the **Q7** cavity. Remarkable **Q7**–protein assemblies, including inter-locked octahedral cages that comprise 24 protein trimers, occurred in the solid state. Cucurbituril clusters appear to be responsible for these assemblies, suggesting a strategy to generate controlled protein architectures.

Over the past fifteen years the donut-shaped cucurbit[n]uril (**Qn**) has emerged as a versatile macrocyclic host for biomolecular recognition^[1,2] with broad applications in protein sensing and regulation.^[3–8] Tight, selective binding to N-terminal aromatic residues^[3,4,7] has paved the way for the development of **Q8**-mediated dimerization,^[9] polymerization^[10] as well as ternary complex formation.^[11] These advances are part of the growing field of supramolecular chemistry with proteins.^[12–14] A wealth of structural evidence is available for protein recognition, and in some cases assembly, by supramolecular receptors.^[4,11,14–21]

Cucurbiturils are attractive hosts for protein recognition due to their selective complexation in aqueous solution, driven by the release of high energy water from the hydrophobic cavity.^[3,4,22–25] For example, **Q7** binds to the N-terminal phenylalanine of insulin with μM affinity in a complex that includes burial of the aromatic ring within the **Q7** cavity and ion-dipole interactions between the N-terminal ammonium and the carbonyl rim of **Q7**.^[4] The larger **Q8** can accommodate the side chains of two aromatic residues.^[3] While this binding mode has featured prominently in numerous **Qn**-protein systems,^[9–11] **Qn** can interact also with lysine, in particular, methylated lysine side chains.^[23,26–31] Mono-, di- and trimethylation of the lysine ammonium (N^ε) are common post translational modifications that occur most notably in histones, with vast ramifications for gene expression.^[32] Methylated lysines (KMe_n) present unique hotspots for recognition by reader proteins that possess an aromatic cage motif. Consequently, synthetic

receptors that recognize KMe_n hold great potential as probes to study biological systems and as inhibitors of protein-protein interactions.^[32–38] **Q7**–KMe_n interactions have been characterized for the amino acids, reveal that the affinity increases dramatically with the degree of methylation.^[28] Recent experiments with a KMe₃-containing histone peptide indicate a ~ 10 -fold drop in K_D relative to the amino acid,^[31] pointing to a favourable contribution by the N^ε group^[32]. To date, there are no literature reports of **Qn**–KMe_n binding with a protein. To address this gap we characterized the interactions of **Q7** with a protein that contains dimethyllysine (KMe₂) and thereby provide a stepping stone to new applications of **Q7** in protein interactions.

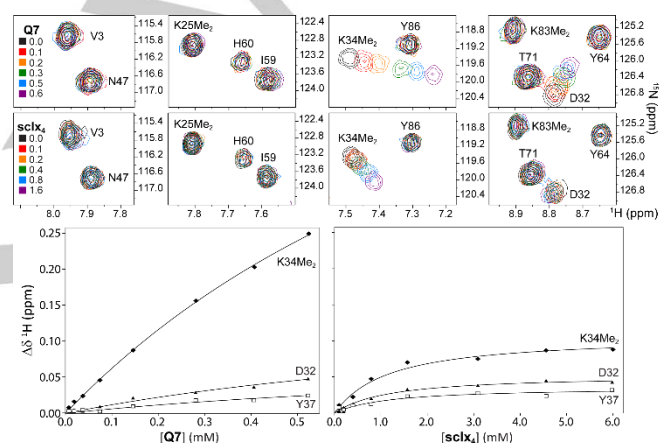


Figure 1. Upper panels. Spectral regions from overlaid ¹H-¹⁵N HSQC spectra of RSL.KMe₂ in the presence of 0–0.6 mM **Q7** or 0–1.6 mM **sclx4**. Each panel provides data on at least one of the four potential binding sites. Resonance V3 is a reporter for S1Me₂ (the N-terminus). Significant chemical shift perturbations were observed for K34Me₂ and the resonances of adjacent residues only. Lower panels. NMR-derived binding curves for complex formation between RSL.KMe₂ and **Q7** or **sclx4**.

Although the affinity of **Q7**–KMe_n complexation increases with the degree of methylation^[28] we studied KMe₂ as this modification is readily accessible in a model protein. *Ralstonia solanacearum* lectin (RSL), an extensively characterized and highly stable ~ 29 kDa trimer with a six-bladed β -propeller topology, was chosen as the model.^[39–42] The protein was chemically dimethylated^[31,41] to yield RSL.KMe₂ with four modified sites, K25Me₂, K34Me₂, K83Me₂ and the N-terminus S1Me₂. Complex formation with **Q7** was investigated by ¹H-¹⁵N HSQC-monitored titrations in 20 mM potassium phosphate, 50 mM NaCl, pH 6.0 (Figure 1). The ¹H-¹⁵N resonances were assigned by comparison to native RSL (Figure S1). A 3.8 mM **Q7** stock solution (SI methods^[44]) was titrated against RSL.KMe₂ and resulted in reproducible, large upfield perturbations of the K34Me₂ amide resonance (Figure 1). The resonances of neighbouring residues W31, D32 and Y37 were affected also. No chemical shift changes occurred at the other possible binding sites (S1Me₂, K25Me₂ or K83Me₂) indicating selectivity for K34Me₂. Control experiments with native RSL

[a] F. Guagnini, Dr. P. M. Antonik, Dr. M. L. Rennie, Prof. Dr. P. B. Crowley
School of Chemistry, National University of Ireland Galway
University Road, Galway (Ireland)
E-mail: peter.crowley@nuigalway.ie

[b] F. Guagnini, Dr. R. Pinalli, Prof. Dr. E. Dalcanale
Dipartimento di Scienze Chimiche della Vita e della Sostenibilità
Ambientale, Università di Parma and INSTM UdR Parma
Parco Area delle Scienze 17/A, 43124 Parma (Italy)

[c] P. O'Byrne, Dr. A. R. Khan
School of Biochemistry and Immunology, Trinity College Dublin,
Dublin 2 (Ireland)

Supporting information for this article is given via a link at the end of the document.

COMMUNICATION

indicated that there was no binding to **Q7** under these conditions (Figure S2). An analysis of $\Delta\delta$ as a function of the ligand concentration yielded shallow binding curves that fit to a K_d of ~ 1 mM (Figure 1 and SI methods). The limited solubility of **Q7** precluded saturation conditions in the NMR experiments. Attempts to obtain thermodynamic information by isothermal titration calorimetry (ITC) were thwarted by the lack of binding heats. Standard titrations of **Q7** into RSL.KMe₂ did not yield usable data. A reverse titration of 5.4 mM RSL.KMe₂ into 0.1 mM **Q7** also gave negligible heat changes (Figure S3). For comparison, NMR titrations were performed with the highly water soluble sulfonatocalix[4]arene (**sclx**₄). Similar to **Q7**,^[28] this anionic receptor binds KMe_n with an affinity that increases with the degree of methylation.^[45] Interestingly, **sclx**₄ also bound selectively to K34Me₂ with a K_d of ~ 1 mM (Figure 1). Minor perturbations at V3 and K83Me₂ indicated that higher concentrations of **sclx**₄ may result in binding at these sites.

Table 1. Crystal structures of RSL.KMe₂ in **Q7**-bound and -free forms.

Space Group / PDB	Res ^[a] (Å)	Precipitant and Buffer	[Q7] / [protein] (mM) ^[b]	Notes
<i>C222</i> ₁ 6F7W	1.3	20 % PEG 3350 0.2 M Na ⁺ Malonate pH 7.0	2.3 / 1.0	Symmetric Q7 No MeFuc
<i>F432</i> 6F7X	2.4	25 % PEG 3350 0.1 M Bis-Tris pH 5.5	1.1 / 1.5	Asymmetric Q7 MeFuc bound
<i>P63</i> 6F7Y	1.6	20 % PEG 3350 0.2 M K ⁺ Formate pH 7.3	2.3 / 1.5	No Q7 bound No MeFuc

[a] See Table S1 for processing and refinement statistics.

[b] Initial concentrations in the crystallization drop.

Further insights into **Q7**-KMe₂ host-guest complexation were obtained by X-ray crystallography. Crystallization was achieved by using a sparse matrix screen (Jena JCSG++). Simple solutions containing ~ 20 % PEG and a buffer (over the pH range 5 - 8) were sufficient to prompt crystal growth. Cubic crystals were obtained when methyl- α -L-fucoside (MeFuc), a ligand to RSL, was included^[46]. Rod shaped crystals also grew in the presence or absence of **Q7** (Figure S4). X-ray data collection was performed both in-house (Rigaku) and at the APS synchrotron (Argonne National Laboratory). The structures were solved by molecular replacement (SI methods, Table S1) and the presence of **Q7** was clear in the electron density maps (Figure S5). The rod shaped crystals proved to be devoid of **Q7**. Two crystal structures of RSL.KMe₂ in the **Q7**-bound and one structure in the **Q7**-free state are reported (Table 1). The latter structure provided useful details on the binding site in the absence of **Q7**.

The **Q7**-bound structures crystallized in the *C222*₁ or *F432* space groups, with an asymmetric unit that comprised one RSL.KMe₂ trimer and three or two **Q7** ligands, respectively. Of the four potential binding sites, **Q7** complexation occurred exclusively at K34Me₂, consistent with the NMR observations (Figure 1). The high selectivity of **Q7** for K34Me₂ can be rationalized in terms of

side chain accessibility^[33]. The accessible surface area of the KMe₂ side chains (calculated as an average from all chains in the three crystal structures) was 160, 240 and 190 Å² for K25Me₂, K34Me₂ and K83Me₂, respectively. K34Me₂ was the most exposed side chain due to its location in a loop (residues 31-37), while K25Me₂ and K83Me₂ are in β -strands. Furthermore, K34Me₂ is flanked by G33 and G35 which confer steric accessibility and backbone mobility. Interestingly, three different modes of **Q7**-K34Me₂ binding were observed. In the *C222*₁ structure, ~ 220 Å² of K34Me₂ was buried in the cavity with both methyl substituents sitting in the central plane of **Q7**. In this orientation the Lys C ^{δ} -C ^{ϵ} bond was intersected by the plane of the rim carbonyl oxygens (Figure 2A). While all three K34Me₂ sites in the RSL.KMe₂ trimer were similar the data at 1.3 Å resolution permitted model building with alternate conformations of K34Me₂ in chains B and C (Figure S6). These conformations suggest that the side chain retained some mobility inside **Q7** and that the cavity was incompletely filled by KMe₂. This packing deficiency may contribute to the lower affinity of **Q7**-KMe₂ with respect to **Q7**-KMe₃.^[28]

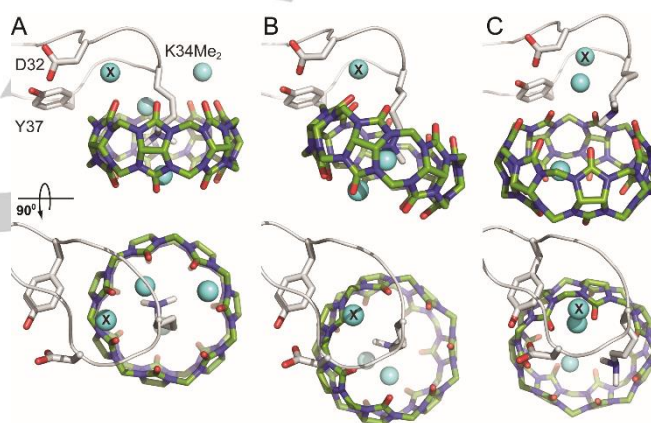


Figure 2. X-ray crystallography reveals complexation of **Q7** at K34Me₂ in RSL.KMe₂. The binding mode of **Q7** was significantly different in space groups (A) *C222*₁ and (B) *F432*. (C) The distal interaction at K34Me₂ in chain B of *F432*. Only the loop residues 31-37 are shown and oriented identically in each structure. Side chains D32, K34Me₂ and Y37 are represented as sticks. Residues 33 and 35 are Gly. Cyan spheres are water molecules and X denotes the conserved water (See Figure S7 for hydrogen bonding pattern). The upper and lower panels are related by a 90° rotation.

The *F432* structure grew from conditions that contained a lower **Q7**:protein ratio compared to *C222*₁ (Table 1) and ligand binding was asymmetric with respect to the RSL.KMe₂ trimer. At chain A, **Q7** bound K34Me₂ (Figure 2B) in a fashion similar to that in the *C222*₁ structure. However, less of the side chain (~ 190 Å²) was buried and the plane of the **Q7** rim carbonyl oxygens intersected the Lys C ^{δ} -C ^{ϵ} bond. At chain B, K34Me₂ formed a distal interaction (~ 130 Å² buried surface) with **Q7** (Figure 2C). This binding mode involved ion-dipole bonds between the ammonium group and two rim carbonyl oxygens (N ^{ζ} ...O=C ~ 3.0 Å). The opposite carbonyl portal formed a similar distal interaction with S1Me₂ of a symmetry related molecule. At chain C, the K34Me₂ was devoid of ligand and the electron density for this side chain was poor, indicative of disorder.

The complete burial of the cationic dimethylammonium group in the hydrophobic cavity of **Q7** raises interesting questions regarding solvation.^[33] Indeed, two water molecules were refined together with the K34Me₂ side chain in the **Q7** cavity (Figure 2). In the C222₁ structure, one water formed a hydrogen bond with the K34Me₂ ammonium group (O^W...N^ζ ~2.7 Å), while simultaneously hydrogen bonded to two rim carbonyl oxygens (O^W...O=C <2.5 Å, Figure S7A). The second water was ~3.4 Å from the closest methyl substituent of the dimethylammonium group, and hydrogen bonded to a lower rim carbonyl, suggesting that the positive charge is partially dissipated to the electronegative rim. Similar interactions were observed in the F432 structure although in this case the water bonded to N^ζ was fully buried and did not interact with the rim carbonyls (Figure 2B). These observations are further intriguing since the cavity of **Q7** can accommodate eight water molecules, the release of which provides the driving force for guest binding.^[2,22,24] This interpretation is based on studies of organic ammonium ions, with encapsulation of the hydrophobic portion inside **Q7** and ion-dipole interactions between the ammonium ion(s) and the rim carbonyls. In the case of KMe₂ encapsulation by **Q7**, six of the waters were displaced and two remaining waters solvated the tertiary ammonium ion inside the cavity (Figure 2).

Water also played a role in mediating **Q7** binding to the protein surface. A conserved water molecule (denoted X, Figures 2 and S7) was refined in each type of binding site and was present also in the **Q7**-free structure. In the C222₁ structure, water X was within hydrogen bond distance of three amide NH groups (D32, K34Me₂ and G35), the carbonyl of G35 and two **Q7** rim carbonyls (Figure S7). In the F432 structure, water X could hydrogen bond with three amides (D32, G33 and K34Me₂) and one **Q7** rim carbonyl. Interestingly, the loop 31-37 had a slightly different conformation at this site such that the amide NH of G35 was flipped out and pointed towards a rim carbonyl to form a unique protein-**Q7** hydrogen bond (N^α...O=C ~3.45 Å).

Despite the high molecular weight (~1.2 kDa) and large surface area (~980 Å²) of **Q7** only 3 or 4 residues on the protein surface were involved directly in ligand complexation. In addition to K34Me₂, neighbouring residues D32, Y37 were the only side chains to form van der Waals contacts with **Q7**. Notably, these two side chains are linked by a hydrogen bond (Oⁿ...O^δ ~2.6 Å) and retained similar positions in all of the binding sites even though the loop, K34Me₂ and **Q7** adopted different conformations (Figures 2 and S7). Apparently, the interaction of **Q7** and the phenol of Y37 were less important than other packing interactions.

Striking examples of protein architectures were observed in the crystal packing. The C222₁ and F432 structures involved trimeric and tetrameric clusters of **Q7**, respectively, suggesting the potential to use the **Q7**-KMe₂ complex as a pivot point for protein assembly (Figures 3 and 4).

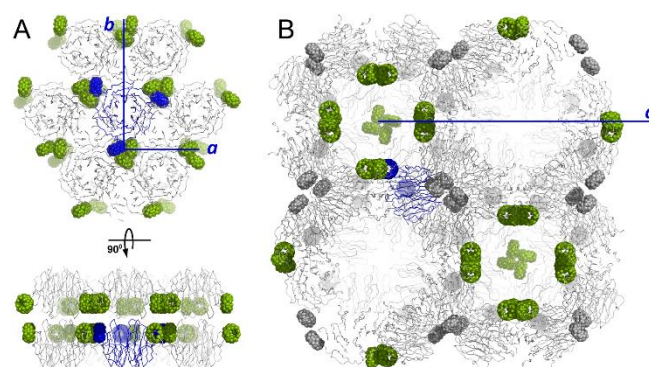


Figure 3. Crystal packing in space groups (A) C222₁ and (B) F432. Note the sheet assembly in C222₁ with **Q7** trimers mediating the packing. In F432 two interlocked cage assemblies were mediated via **Q7** tetramers (green). The distal binding **Q7** (see Figure 2C) is grey. Protein and ligand are shown as ribbons and spheres, respectively. The asymmetric unit and the unit cell axes are indicated in blue. Note that axis *a* is (A) ~50 or (B) ~200 Å.

Qn clusters are well-established in the literature, involving at least one CH...O=C bond between pairs of macrocycles,^[47-49] and a supramolecular triangle was reported recently for **Q8**.^[48] In C222₁ (Figure 3A), sheets of trigonally-arrayed RSL.KMe₂ trimers are arranged around **Q7** trimers (Figure 4A). In addition to six CH...O=C interactions, each **Q7** acted as a bidentate ligand to a central sodium ion. The cation was complexed by ion-dipole bonds from two of the rim carbonyls (Na⁺...O=C ~2.5 Å) resulting in an octahedral coordination geometry. Salts of alkali metals can increase **Qn** solubility through coordination of the rim carbonyls.^[2,50] It is tempting to conclude that sodium was critical to the growth of the C222₁ crystal considering that **Q7**-free crystals grew from similar conditions in which sodium malonate was replaced by potassium formate (Table 1).

F432 is a rare space group characteristic of protein cages such as ferritin.^[51] Remarkably, **Q7** at chain A mediated four-fold symmetric junctions to form a porous assembly of interlocked cages with 24 RSL.KMe₂ trimers disposed at the vertices of a regular octahedron (Figures 3B and 4B). This cage-like assembly has an internal diameter of ~6 nm, comparable to that of ferritin.^[51] In addition to the lower **Q7**:protein ratio, the crystallization pH was also lower (relative to C222₁, Table 1) and may have favoured cage formation as the net charge on the protein switched from anionic to cationic (RSL pI ~6.8). Interestingly, the **Q7**-**Q7** interfaces (Figure 4) buried ~300 and ~240 Å² of surface (per **Q7**) in the C222₁ and F432 structures, while **Q7**-protein contacts buried ~240 Å² of the ligand surface. It can be assumed that the relatively low water solubility of **Q7** is conducive to the formation of **Q7**-mediated protein architectures. Furthermore, the **Q7** clusters at protein-protein interfaces may be an extension on the theme of macrocyclic molecular glues for protein assembly and crystallization^[19-21].

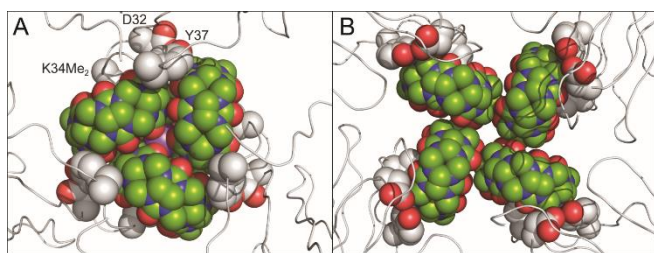


Figure 4. Trimeric and tetrameric cucurbituril clusters in space groups (A) C_{2221} and (B) F_{432} in which **Q7-Q7** packing buried ~ 300 or ~ 240 Å² of ligand surface, respectively. In C_{2221} the trimeric **Q7** formed an octahedral complex with a sodium cation (central, purple sphere). Side chains D32, K34Me₂ and Y37 are represented as spheres.

Supramolecular building blocks are increasingly popular as receptors for protein binding and assembly.^[12-14] Examples include protein oligomerization mediated by calixarenes^[15,16] and foldamers.^[17] Anionic calixarenes have proven particularly useful for the assembly of cationic proteins.^[16,19,21] The binding of **Qn** to N-terminal aromatic residues is an established route to controlled protein interactions.^[4,9-11] Programmable assembly of dimers^[9] and polymers^[10] can be achieved *via* the combination of **Q8** with proteins that bear an N-terminal phenylalanine. This repertoire has been expanded now to include **Q7-KMe₂** complexation and assembly. Contrary to amino acid^[28] and peptide studies^[31] we observed a modest affinity for the **Q7-KMe₂** interaction in the model protein RSL.KMe₂ (Figure 1). Nevertheless, the affinity was sufficient to effect protein assembly in the solid state, with **Q7-Q7** packing playing pivotal roles (Figures 3 and 4). The poor water solubility of **Q7** is apparently advantageous in this regard. The pronounced selectivity of **Q7** for the most exposed KMe₂ (Figures 1 and 2) points to a simple strategy of engineered protein assemblies based on **Q7-KMe₂** complexation. Finally, the tighter **Q7-KMe₃** interaction^[28] suggests that this motif can be employed to greater advantage than **Q7-KMe₂** in protein assembly.

Acknowledgements

This research was supported by NUI Galway and Science Foundation Ireland (grants 13/ERC/B2912 and 13/CDA/2168 to PBC) and by University of Parma intramural funding (PhD fellowship to FG). B. Harhen and R. Doohan are thanked for assistance with mass spectrometry and NMR spectroscopy, respectively. We acknowledge the staff of NE-CAT at the Advanced Photon Source for assistance with data collection.

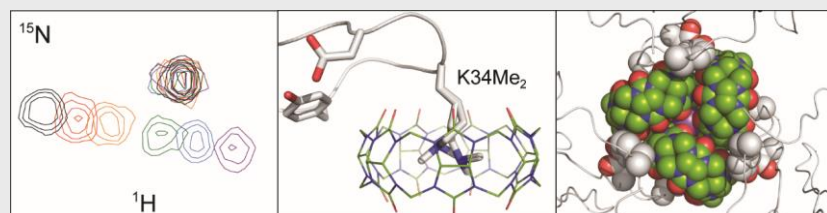
Keywords: cucurbituril • desolvation • macrocycle • molecular recognition • supramolecular chemistry

- [1] J. W. Lee, S. Samal, N. Selvapalam, H. J. Kim, K. Kim, *Acc. Chem. Res.* **2003**, *36*, 621-630.
 [2] S. J. Barrow, S. Kaseera, M. J. Rowland, J. del Barrio, O. A. Scherman, *Chem. Rev.* **2015**, *115*, 12320-12406.
 [3] L. M. Heitmann, A. B. Taylor, P. J. Hart, A. R. Urbach, *J. Am. Chem. Soc.* **2006**, *128*, 12574-12581.

- [4] J. M. Chinai, A. B. Taylor, L. M. Ryno, N. D. Hargreaves, C. A. Morris, P. J. Hart, A. R. Urbach, *J. Am. Chem. Soc.* **2011**, *133*, 8810-8813.
 [5] J. W. Lee, M. H. Shin, W. Mobley, A. R. Urbach, H. I. Kim, *J. Am. Chem. Soc.* **2015**, *137*, 15322-15329.
 [6] S. Sonzini, A. Marcozzi, R. J. Gubeli, C. F. van der Walle, P. Ravn, A. Herrmann, O. A. Scherman, *Angew. Chem. Int. Ed.* **2016**, *55*, 14000-14004.
 [7] W. Li, A. T. Bockus, B. Vinciguerra, L. Isaacs, A. R. Urbach, *Chem. Commun.* **2016**, *52*, 8537-8540.
 [8] J. Murray, J. Sim, K. Oh, G. Sung, A. Lee, A. Shrinidhi, A. Thirunarayanan, D. Shetty, K. Kim, *Angew. Chem. Int. Ed.* **2017**, *56*, 2395-2398.
 [9] H. D. Nguyen, D. T. Dang, J. L. van Dongen, L. Brunsveld, *Angew. Chem. Int. Ed.* **2010**, *49*, 895-898.
 [10] C. Hou, J. Li, L. Zhao, W. Zhang, Q. Luo, Z. Dong, J. Xu, J. Liu, *Angew. Chem. Int. Ed.* **2013**, *52*, 5590-5593.
 [11] P. J. de Vink, J. M. Briels, T. Schrader, L. G. Milroy, L. Brunsveld, C. Ottmann, *Angew. Chem. Int. Ed.* **2017**, *56*, 8998-9002.
 [12] F. G. Klärner, T. Schrader, *Acc. Chem. Res.* **2013**, *46*, 967-978.
 [13] Q. Luo, C. Hou, Y. Bai, R. Wang, J. Liu, *Chem. Rev.* **2016**, *116*, 13571-13632.
 [14] S. van Dun, C. Ottmann, L. G. Milroy, L. Brunsveld, *J. Am. Chem. Soc.* **2017**, *139*, 13960-13968.
 [15] R. E. McGovern, H. Fernandes, A. R. Khan, N. P. Power, P. B. Crowley, *Nat. Chem.* **2012**, *4*, 527-533.
 [16] R. E. McGovern, A. A. McCarthy, P. B. Crowley, *Chem. Commun.* **2014**, *50*, 10412-10415.
 [17] J. Buratto, C. Colombo, M. Stupfel, S. J. Dawson, C. Dolain, B. Langlois d'Estaintot, L. Fischer, T. Granier, M. Laguerre, B. Gallois, I. Huc, *Angew. Chem. Int. Ed.* **2014**, *53*, 883-887.
 [18] D. Bier, S. Mittal, K. Bravo-Rodriguez, A. Sowislok, X. Guillory, J. Briels, C. Heid, M. Bartel, B. Wettig, L. Brunsveld, E. Sanchez-Garcia, T. Schrader, C. Ottmann, *J. Am. Chem. Soc.* **2017**, *139*, 16256-16263.
 [19] M. L. Rennie, A. M. Doolan, C. L. Raston, P. B. Crowley, *Angew. Chem. Int. Ed.* **2017**, *56*, 5517-5521.
 [20] A. M. Doolan, M. L. Rennie, P. B. Crowley, *Chem. Eur. J.* **2018**, *24*, 984-991.
 [21] J. M. Alex, M. L. Rennie, S. Volpi, F. Sansone, A. Casnati, P. B. Crowley, *Cryst. Growth Des.* **2018**, *18*, 2467-2473.
 [22] F. Biedermann, V. D. Uzunova, O. A. Scherman, W. M. Nau, A. De Simone, *J. Am. Chem. Soc.* **2012**, *134*, 15318-15323.
 [23] Y. Wang, J. R. King, P. Wu, D. L. Pelzman, D. N. Beratan, E. J. Toone, *J. Am. Chem. Soc.* **2013**, *135*, 6084-6091.
 [24] F. Biedermann, W. M. Nau, H. J. Schneider, *Angew. Chem. Int. Ed.* **2014**, *53*, 11158-11171.
 [25] D. Sigwalt, M. Šekutor, L. Cao, P. Y. Zavaliij, J. Hostaš, H. Ajani, P. Hobza, K. Mlinarić-Majerski, R. Glaser, L. Isaacs, *J. Am. Chem. Soc.* **2017**, *139*, 3249-3258.
 [26] D. M. Bailey, A. Hennig, V. D. Uzunova, W. M. Nau, *Chem. Eur. J.* **2008**, *14*, 6069-6077.
 [27] H. Zhang, M. Grabenauer, M. T. Bowers, D. V. Dearden, *J. Phys. Chem. A* **2009**, *113*, 1508-1517.
 [28] M. A. Gamal-Eldin, D. H. Macartney, *Org. Biomol. Chem.* **2013**, *11*, 488-495.

- [29] J. W. Lee, H. H. Lee, Y. H. Ko, K. Kim, H. I. Kim, *J. Phys. Chem B* **2015**, *119*, 4628-4636.
- [30] E. Kovalenko, M. Vilaseca, M. Díaz-Lobo, A. N. Masliy, C. Vicent, V. P. Fedin, *J. Am. Soc. Mass Spectrom.* **2016**, *27*, 265-276.
- [31] J. Lee, L. Perez, Y. Liu, H. Wang, R. J. Hooley, W. Zhong, *Anal. Chem.* **2018**, *90*, 1881-1888.
- [32] J. E. Beaver, M. L. Waters, *ACS Chem. Biol.* **2016**, *11*, 643-653.
- [33] R. E. McGovern, B. D. Snarr, J. A. Lyons, J. McFarlane, A. L. Whiting, I. Paci, F. Hof, P. B. Crowley, *Chem. Sci.* **2015**, *6*, 442-449.
- [34] H. Peacock, C. C. Thinnis, A. Kawamura, A. D. Hamilton, *Supramol. Chem.* **2016**, *28*, 575-581.
- [35] R. Pinalli, G. Brancatelli, A. Pedrini, D. Menozzi, D. Hernández, P. Ballester, S. Geremia, E. Dalcanale, *J. Am. Chem. Soc.* **2016**, *138*, 8569-8580.
- [36] I. N. Gober, M. L. Waters, *J. Am. Chem. Soc.* **2016**, *138*, 9452-9459.
- [37] Y. Liu, L. Perez, A. D. Gill, M. Mettry, L. Li, Y. Wang, R. J. Hooley, W. Zhong, *J. Am. Chem. Soc.* **2017**, *139*, 10964-10967.
- [38] N. Bontempi, E. Biavardi, D. Bordiga, G. Candiani, I. Alessandri, P. Bergese, E. Dalcanale, *Nanoscale* **2017**, *9*, 8639-8646.
- [39] N. Kostlánová, E. P. Mitchell, H. Lortat-Jacob, S. Oscarson, M. Lahmann, N. Gilboa-Garber, G. Chambat, M. Wimmerová, A. Imberty, *J. Biol. Chem.* **2005**, *280*, 27839-27849.
- [40] J. Arnaud, K. Tröndle, J. Claudinon, A. Audfray, A. Varrot, W. Römer, A. Imberty, *Angew. Chem. Int. Ed.* **2014**, *53*, 9267-9270.
- [41] P. M. Antonik, A. N. Volkov, U. N. Broder, D. Lo Re, N. A. J. van Nuland, P. B. Crowley, *Biochemistry*, **2016**, *55*, 1195-1203.
- [42] P. M. Antonik, A. M. Eissa, A. R. Round, N. R. Cameron, P. B. Crowley, *Biomacromol.* **2016**, *17*, 2719-2725.
- [43] S. T. Larda, M. P. Bokoch, F. Evanics, R. S. Prosser, *J. Biomol. NMR.* **2012**, *54*, 199-209.
- [44] S. Yi, A. E. Kaifer, *J. Org. Chem.* **2011**, *76*, 10275-10278.
- [45] C. S. Beshara, C. E. Jones, K. D. Daze, B. J. Lilgert, F. Hof, *ChemBioChem* **2010**, *11*, 63-66.
- [46] MeFuc binding was not perturbed by Q7 binding, see Figure S8.
- [47] S. Lim, H. Kim, N. Selvapalam, K. J. Kim, S. J. Cho, G. Seo, K. Kim, *Angew. Chem. Int. Ed.* **2008**, *47*, 3352-3355.
- [48] D. Bardelang, K. Banaszak, H. Karoui, A. Rockenbauer, M. Waite, K. Udachin, J. A. Ripmeester, C. I. Ratcliffe, O. Ouari, P. Tordo, *J. Am. Chem. Soc.* **2009**, *131*, 5402-5404.
- [49] D. Bardelang, K. A. Udachin, D. M. Leek, J. C. Margeson, G. Chan, C. I. Ratcliffe, J. A. Ripmeester, *Cryst. Growth Des.* **2011**, *11*, 5598-5614.
- [50] Y.-M. Jeon, J. Kim, D. Whang, K. Kimoon, *J. Am. Chem. Soc.* **1996**, *118*, 9790-9791.
- [51] B. Maity, S. Abe, T. Ueno, *Nat. Commun.* **2017**, *8*, 14820.

COMMUNICATION



Francesca Guagnini, Paweł M. Antonik,
Martin L. Rennie, Peter O'Byrne, Amir R.
Khan, Roberta Pinalli, Enrico Dalcanale,
and Peter B. Crowley*

Page No. – Page No.

**Cucurbit[7]uril–Dimethyllysine
Recognition in a Model Protein**